Studying genomic processes at the single-molecule level: introducing the tools and applications

David Dulin, Jan Lipfert, M. Charl Moolman and Nynke H. Dekker

Abstract | To understand genomic processes such as transcription, translation or splicing, we need to be able to study their spatial and temporal organization at the molecular level. Single-molecule approaches provide this opportunity, allowing researchers to monitor molecular conformations, interactions or diffusion quantitatively and in real time in purified systems and in the context of the living cell. This Review introduces the types of application of single-molecule approaches that can enhance our understanding of genome function.

Replisome
A multi-protein complex that carries out DNA replication.

Department of Bionanoscience, Kavli Institute of Nanoscience, Delft University of Technology, Lorentzweg 1, 2628 CJ Delft, The Netherlands. Correspondence to N.H.D. e-mail: n.h.dekker@tudelft.nl
doi:10.1038/nrg3316
Published online 14 November 2012; corrected 23 November 2012

Cells rely on the correct readout, maintenance, repair and replication of genomic information. These are processes that involve a stunning variety of carefully coordinated and regulated molecular actors. Although many of the important players were identified decades ago, quantitative and mechanistic insight into their actions and interactions remains a challenge that has attracted scientists from disciplines that neighbour molecular biology and biochemistry, such as biophysics, bioinformatics and nanoscience.

To obtain quantitative insight into genomic processes, probing at the single-molecule level has proved to be very successful. For example, single-molecule methods can detect transient intermediates or rare events that are masked when ensemble techniques that average the behaviour of a large number of molecules are used. Single-molecule measurements require techniques that are capable of probing biological material with nanometre-scale spatial and millisecond temporal resolution. Furthermore, techniques must be compatible with aqueous environments, as genomic processing takes place in the context of the living cell. Single-molecule methods now exist that reach this capability in a range of environments from simple saline solutions used for *in vitro* studies to the densely crowded environment of the living cell.

Using single-molecule approaches, a wealth of quantitative information on the activity of proteins involved in genome processing has been obtained in recent years. For example, experiments have allowed us to distinguish the different stepping motions used by helicases, to witness the progress of RNA polymerase (RNA Pol) base pair by base pair and to follow the activity of the replisome in live cells in real time, to name but a few. Complementing excellent studies using bulk approaches that for reasons of space we cannot detail in this Review, the results of single-molecule studies have provided us with detailed mechanistic insight into the functions and mechanisms of motor proteins and have even found a major commercial application in single-molecule DNA-sequencing approaches (recently reviewed in REF. 1). Yet the field is by no means mature. Single-molecule studies are increasingly going 'beyond single molecules'. Experiments are beginning to address multi-component systems and their mutual interactions: for example, they study more than the interaction of a single protein with DNA. This development has gone hand-in-hand with the ability of techniques to detect different molecular components simultaneously and to carry out many single-molecule experiments in parallel, allowing high-throughput data collection while still resolving the fundamental behaviour of individual molecules.

In this Review, we provide an introduction to single-molecule approaches to study genomic processes and highlight examples of insights obtained using these methods. We first focus on transcription and translation, then highlight recent progress in studying RNA export and splicing and conclude by demonstrating the dynamics of protein–protein interactions in replication. Other areas of genome processing that have benefited from the single-molecule approach include DNA repair and recombination, and these have been reviewed elsewhere[2,3]. As it is possible to monitor the motion of a single biological molecule both *in vitro* as well as inside a living cell, we compare and contrast genome processing in these two different contexts. Throughout, we indicate how specific insights rely on the capabilities afforded by single-molecule methods.

Tethered particle motion (TPM). A single-molecule technique that uses tethered beads to study biological molecules in the absence of any externally applied force. Changes in the average position of the bead can report on changes in tether length and hence on enzyme activity.

Measuring at the single-molecule limit

Although achieving the single-molecule limit is in and of itself fairly straightforward (for example, by sufficient dilution of a molecular sample), the challenge has always been how to observe or to manipulate single molecules. Signals are inevitably weak, and the measurement apparatus is always macroscopic. Techniques such as electron microscopy[4–6] and patch clamp detection[7] were early advances along these lines. In this Review, we focus on the principal single-molecule techniques that are used for the study of genome processing: namely, force spectroscopy (BOX 1) and fluorescence spectroscopy (BOX 2). The developments of atomic force microscopy, video-based tethered particle motion (TPM) and optical and magnetic tweezers have formed the key methodological advances in force spectroscopy. Optical and magnetic tweezers in particular have succeeded in combining great flexibility in terms of molecular manipulation with

Box 1 | **Single-molecule force-manipulation techniques**

A range of techniques can be used to apply forces (and, in some cases, torques) to individual molecules or molecular assemblies[115–117]. These single-molecule manipulation techniques rely on specifically attaching the extremities of the molecule (or molecules) of interest between a surface and a force transducer: for example, to a magnetic or dielectric bead or a cantilever used in atomic force microscopy (AFM)[117]. Specific attachment is accomplished by means such as biotin–streptavidin linkage, thiol bonds or antibodies.

In magnetic tweezers (panel **a** of the figure), permanent or electrical magnets are used to manipulate surface-tethered magnetic beads by controlling the external fields. The force (shown by the 'F' in the figure) on the magnetic beads depends on the gradient of the magnetic field[118]. In addition to forces, magnetic tweezers can also routinely apply torques by rotating the magnetic fields[82,119]. In flow–stretch experiments (panel **b**), liquid flow exerts drag forces on tethered beads[120]. The force can be controlled by adjusting the flow rate. In AFM, forces are applied to individual molecules tethered between a functionalized AFM cantilever and a surface[117,121] (panel **c**). Optical tweezers hold a dielectric particle or bead in the focus of an intense laser beam[117,122,123] (panels **d**–**f**). Common optical tweezers geometries have one end of a nucleic acid tether attached to a bead held in an optical trap while the other end is attached to either the surface (panel **f**) to another optically trapped bead (panel **e**, a so-called dumb-bell or dual-bead assay) or to a bead held in a micropipette (panel **d**). In flow–stretch and magnetic tweezers set-ups, the tether extension is typically monitored by charge-coupled-device-camera-based tracking of the bead positions. In optical tweezers or AFM, the laser signal is usually read out with a position-sensitive device or quadrant photodiode[121,122]. Flow–stretch and magnetic tweezers intrinsically operate in constant force mode: that is, for a given setting of the flow speed or magnetic fields, the stretching force exerted on the tether is (nearly) constant. By contrast, optical tweezers and AFM intrinsically control the extension by controlling the position of the optical trap or cantilever. Constant extension techniques can be operated in (approximately) constant force mode by using feedback control or by exploiting trap nonlinearities[124]. All four techniques can apply forces in the pico-Newton (pN) to tens of pN range (panel **g**), which is suitable for studying biological processes at the molecular scale (for example, the stall force for polymerases is in the range of 10 pN). AFM measurements are at the high-force end on this scale, whereas magnetic tweezers are particular well-suited to accurately applying and measuring very low forces[117].

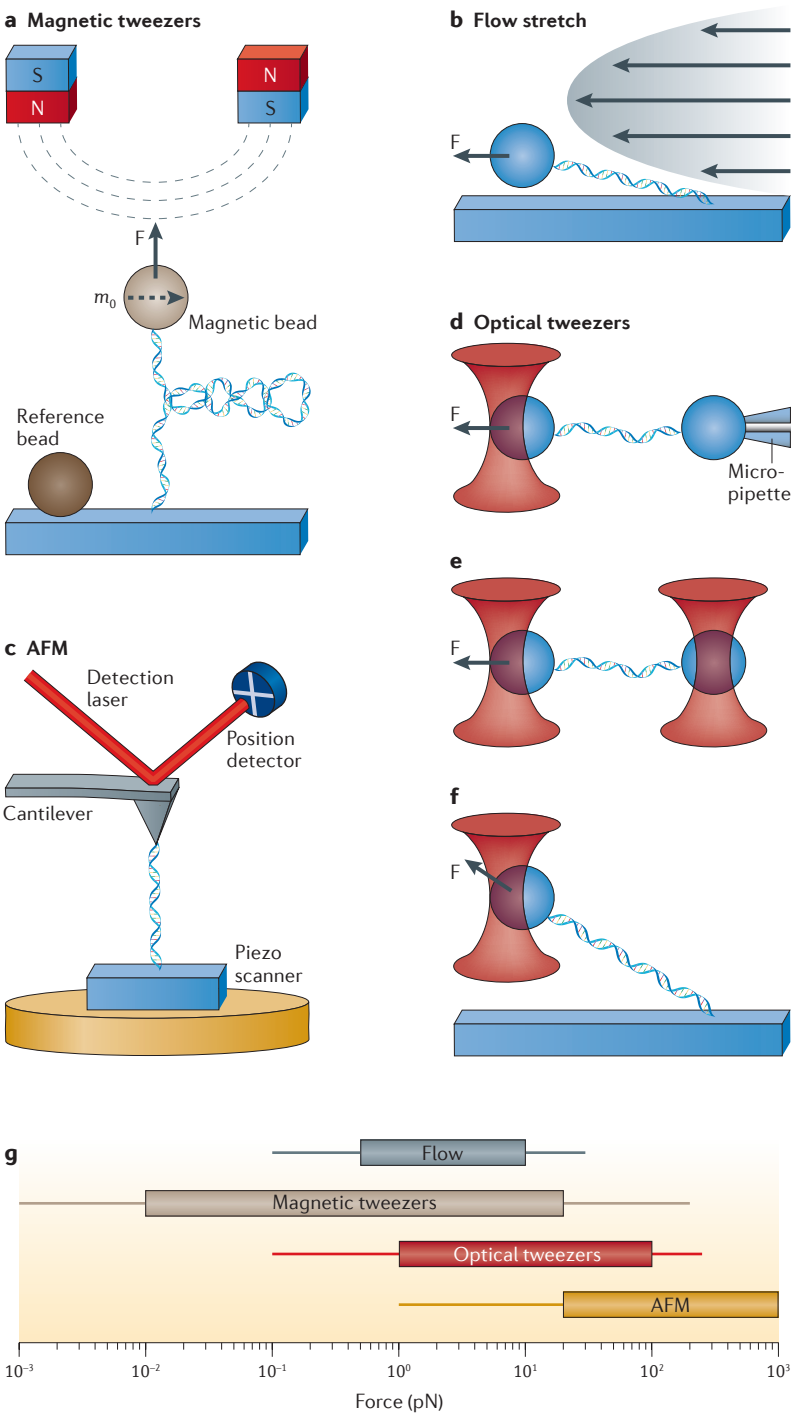

Box 2 | **Fluorescence microscopy**

Fluorescence microscopy is a versatile, widely used tool for studying biological processes both *in vivo* and *in vitro*. It relies on the fact that molecules can emit light after they have absorbed it at a different (typically shorter) wavelength. The efficiency of this process depends on the type of molecule used. Many different kinds of fluorescent probes are available and each has its own specific set of characteristics[125–127]. They can be divided into two broad classes: fluorescent proteins, which are a common choice for live-cell imaging[126], given their high specificity; and organic dyes, which have a greater brightness but suffer from lower specificity inside living cells.

In addition to the choice of the fluorophore, an important consideration is the excitation method used. Panel **a** of the figure shows four frequently used excitation strategies: wide-field, confocal, total internal reflection fluorescence (TIRF) microscopy and zero-mode waveguides (ZMWs). These methods differ from one another by the excitation volume, shown here in green. In wide-field microscopy, the sample is excited by a nearly collimated light beam. Out-of-focus fluorophores are also excited, increasing the background noise and rendering probe localization more difficult. Confocal microscopy reduces the excitation volume by using a focused laser beam and a spatial filter in front of the detector to eliminate any out-of-focus fluorescence light. Both TIRF microscopy and ZMWs use evanescent waves to reduce the excitation volume, making it possible to excite only molecules that are within ~100 nm of the surface and as such substantially reducing the background fluorescence[128]. In ZMWs, the excitation volume in the imaging plane is further restricted compared to TIRF microscopy by making use of nanofabricated structures with typical dimensions of ~100 nm (inset). An important parameter in determining the most suitable technique is the required concentration of fluorescently labelled components. For example, physiologically relevant ligand conditions are preferred for studies of enzymatic activity. Higher concentrations of a fluorescently labelled ligand result in higher background fluorescence and, consequentially, an increased need to reduce the excitation and detection volumes. On the left of panel **a** are indicated the typical concentrations of fluorophore-labelled molecules (ranging from pM to μM) that can be investigated with these respective techniques.

Fluorescence excitation of individual fluorophores gives rise to diffraction-limited spots that can be detected with sensitive detectors, typically electron-multiplying charge-coupled-device cameras or photodiodes. The position of these fluorescent foci can be determined using single-molecule localization methods with an uncertainty in the nanometre range (depending on the signal-to-noise ratio of the measurement). Single-molecule localization involves fitting the spatially distributed intensity of the detected fluorescence spot to a mathematical function (typically a Gaussian function) to determine its centre (panel **b**)[129–132]. The newly developed super-resolution techniques (which were recently reviewed in REFS 133,134) have developed ways of successively localizing neighbouring molecules to build up an image with resolution beyond that permitted by the Rayleigh criterion.

The preferred microscopy method is highly dependent on the type of investigation. Low background techniques, such as TIRF and confocal microscopy, are commonly used to probe three-dimensional conformational changes. This can be done in combination with Förster (fluorescence) resonance energy transfer (FRET). FRET is based on the non-radiative energy transfer between so-called donor (green) and acceptor (red) fluorophores in close proximity[17] (panel **c**). Following excitation, the donor molecule can non-radiatively transfer its energy to a sufficiently close acceptor molecule, resulting in a decrease in the (green) donor fluorescence signal and a concomitant increase in the (red) acceptor fluorescence signal. Monitoring the degree of energy transfer reports on the distance and dynamics of intra- and intermolecular interactions on the sub-10 nm scale[135].

Please note that the diagrams are not drawn to scale and are meant for illustration purposes only. AU, absorbance units.

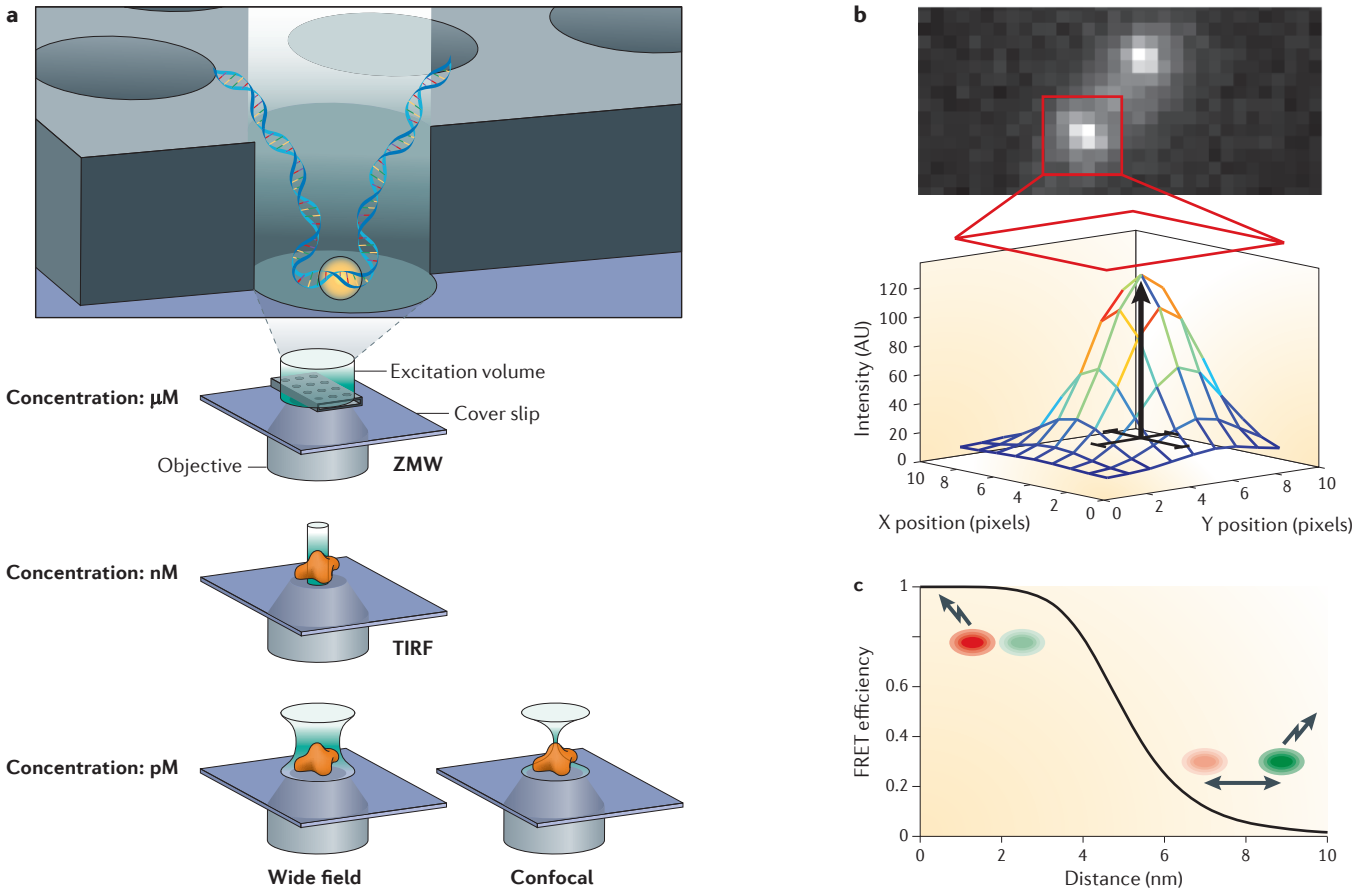

high spatial and temporal resolution. The development of optical methods to visualize individual molecules[8,9], the introduction of genetically encodable fluorophores, such as GFP[10], and the introduction of fast detectors and sensitive cameras have been key to the widespread use of fluorescence spectroscopy. Indeed, using this approach it has now become routine to monitor the motion of individual molecules of different types within living cells.

There are many possible reasons for choosing single-molecule methods to study genomic processes. Most obviously, they allow re-examination of known biological processes in real time directly as they occur. In many cases, the high spatial and temporal resolution afforded by single-molecule techniques has made it possible to gain unique insight into enzymatic dynamics. This has particularly been the case for studies of genome processing, in which the ~3 Å base pair spacing sets a critical length scale. Importantly, single-molecule techniques provide inherent synchronization, in the sense that the starting point of enzymatic activity is always known. Hence, the signals of molecular activities are not affected by averaging asynchronous events. For example, studies of the repetitive cycles of elongation in transcription, translation and replication benefit from this lack of averaging. Additionally, when studying biological systems of considerable compositional complexity (for example, the ribosome and its associated factors), single-molecule techniques can permit the selection, and hence the study, of correctly assembled complexes only. Finally, the sheer diversity of parameters that can be measured by single-molecule techniques — such as enzymatic stall forces[11], backwards motion of an enzyme along a DNA template[12], the presence of friction during enzyme motion[13,14] and many more — has also played an important part in their wide acceptance.

Transcription

Our understanding of the key molecular motor that powers transcription, RNA Pol, has been greatly advanced by single-molecule methods. Following the lead of initial single-molecule work on *Escherichia coli* RNA Pol[15], studies have primarily focused on bacterial systems, but more recently eukaryotic RNA Pol II has also been examined.

Initiation. In bacteria, an important step in transcription initiation is the transition from the so-called closed promoter complex to the open promoter complex, a process in which the RNA polymerase holoenzyme (RNA Pol holoenzyme) locally melts the DNA. The value of *in vitro* multicolour single-molecule total internal reflection fluorescence (TIRF)-microscopy-based assays (see panel **a** of the figure in BOX 2) is shown by a study that sheds light on the various substeps of this transition and their dynamics for the case of transcriptional regulation by σ54 (REF. 16). Such an approach is widely applicable and provides large data sets that report on the association and dissociation of multiple, differentially labelled molecules in a single experiment. The low dissociation rates between σ54, *E. coli* RNA Pol and DNA mean that fairly low concentrations of labelled molecules could be used (because the molecules could 'wait' for the arrival of a labelled component), and thus this facilitated the observation of individual molecules using TIRF microscopy (BOX 2). The authors observed that the transition from an unbound *E. coli* RNA Pol to a closed promoter complex can be decomposed into two substeps, each of which is characterized by its own lifetime, and the rate of the second substep is rate-limiting for the overall transition into the open promoter complex. They further determined that in the presence of competing processes, such as dissociation, on average 30 attempts are necessary for *E. coli* RNA Pol to reach the open promoter complex. Interestingly, these studies showed that the dynamics of the σ54-dependent initiation pathway differ substantially from those of the more common σ70-dependent pathway but closely resemble eukaryotic pathways.

Single-molecule Förster (fluorescence) resonance energy transfer (smFRET)[17] (see panel **c** of the figure in BOX 2) and magnetic tweezers[18] (see panel **a** of the figure in BOX 1) have been used to distinguish between three different models proposed for the transition of the *E. coli* RNA Pol holoenzyme from initiation into elongation: transient excursion (in which *E. coli* RNA Pol diffuses back and forth on the DNA between subsequent abortive initiations); inchworming (in which *E. coli* RNA Pol stretches further along on the DNA template with each successive ribonucleotide incorporation, followed by subsequent release); and scrunching (in which the DNA transcription bubble increases in size with each successive ribonucleotide incorporation, followed by subsequent release). To probe these different possibilities, smFRET was used with several dye-labelling strategies[17] (FIG. 1A,B). For example, labelling the trailing edge of *E. coli* RNA Pol and the upstream template DNA enabled the authors to monitor the relative distance between these molecules; as this distance did not change, they were able to discard the transient excursion model. Labelling the trailing edge of *E. coli* RNA Pol and the DNA downstream from the promoter revealed that their relative distance was unaltered during the transition into elongation, hence the inchworming model was similarly ruled out. Finally, by labelling the leading edge of *E. coli* RNA Pol and the upstream DNA, the authors showed that 7–9 base pairs are scrunched before elongation. A study that analysed promoter unwinding on supercoiled DNA in magnetic tweezers reached similar conclusions[18]. Eukaryotic RNA Pol II initiation has also been studied using an smFRET-based triangulation approach to observe the transition from the open complex conformation into elongation[19]. By labelling RNA Pol II, the DNA template and several transcription factors, the authors observed a large conformational change of the initiation complex during the transition from initiation into elongation, which is facilitated by the intrinsic flexibility of eukaryotic transcription factor IIB (TFIIB)[19].

Elongation. Single-molecule studies of elongation have revealed the rich dynamics of nucleotide incorporation, in particular, the presence of various kinds of pauses, and here we note a few examples to show the types of application of these methods. The first *in vitro* single-molecule

Evanescent waves
Parallel optical waves with an exponentially decaying intensity that occur near a surface when incident light impinges at an angle greater than the critical angle for refraction.

Rayleigh criterion
Quantifies the minimum resolvable distance between two objects that fluoresce at the same wavelength. This distance equals roughly half the wavelength of light.

RNA polymerase holoenzyme
The initiation complex composed of the RNA polymerase core enzyme and the σ-initiation factor.

σ54
One of the initiation factors that can bind to *Escherichia coli* RNA polymerase during initiation to allow it to recognize a specific promoter sequence.

σ70
The most common and most widely studied initiation factor that can bind to *Escherichia coli* RNA polymerase during initiation to allow it to recognize a specific promoter sequence.

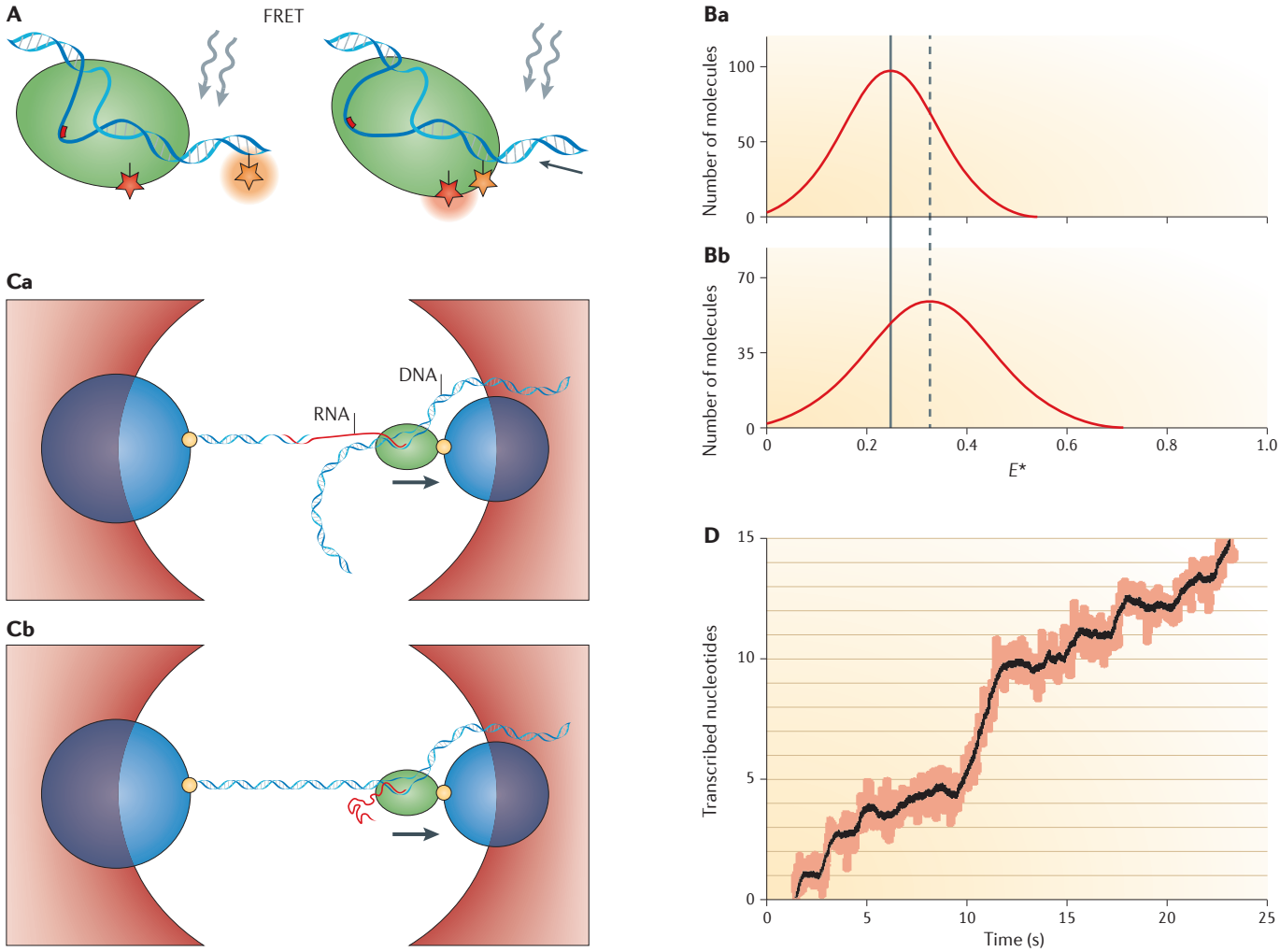

Figure 1 | **Studies of RNA polymerase at the single-molecule level.** **A** | A schematic of a small-molecule Förster (fluorescence) resonance energy transfer (smFRET) experiment in which the polymerase and the DNA template strand are labelled by an acceptor and a donor fluorophore, respectively[17]. **B** | Representation of the results from this experiment. At the start of the reaction, the FRET signal is weak (**a**). Subsequent advancement by *Escherichia coli* RNA polymerase (RNA Pol) results in higher FRET efficiency, as shown by the shift in the distribution (**b**). Even small structural changes in the *E. coli* RNA Pol can be monitored in this way. **C** | An example of a force spectroscopy experiment that relies on a dumb-bell assay in an optical trap to monitor transcription. The direction of *E. coli* RNA Pol motion is indicated by the arrows. Note that force can applied in different ways: to the upstream DNA template as an assisting force (**a**; a force applied to the downstream DNA template (not shown) would provide an opposing force); or to the synthesized mRNA (**b**). **D** | The observation of transcription elongation by a single *E. coli* RNA Pol at base-pair resolution. Raw data are shown in red, and smoothed data are shown in black. The horizontal lines are spaced by the distance between nucleotides. *E**, efficiency of donor–acceptor energy transfer. Data in panels **Ba** and **Bb** are taken from REF. 17. Panel **C** is modified, with permission, from REF. 34 © (2008) Elsevier. Panel **D** is modified, with permission, from REF. 20 © (2005) Macmillan Publishers Ltd. All rights reserved.

studies of RNA Pol (which used TPM) revealed heterogeneities in RNA Pol velocity[15]. Since then, studies of elongation have primarily relied on optical tweezers (FIG. 1C) and have benefited from the high spatiotemporal resolution that can now be achieved — single base pairs in a 1-second bandwidth[20] (FIG. 1D). Such studies of transcription dynamics have highlighted how RNA Pol progression is interrupted by different kinds of pauses[21–26]. For example, studies in which an assisting force was applied to *E. coli* RNA Pol using optical tweezers (FIG. 1Ca) showed that pauses occur at rates that are sequence- and force-dependent and have durations that are exponentially distributed and independent of the magnitude of the applied force[22,27]. Such exponentially distributed pauses could be modulated by the presence of co-transcriptional factors, such as NusG (which decreases the pause density[28]) and NusA (which increases the pause density[27]). Conversely, the application of an opposing force on *E. coli* RNA Pol resulted in the observation of long pauses attributed to backtracking[23,29]. Backtracking

involves backwards diffusion of RNA Pol on its template while part of the mRNA is extruded, and it is facilitated by nucleotide misincorporation[23]. However, studies of *E. coli* RNA Pol disagree on the relative contribution of backtracking pauses versus exponentially distributed pauses[23,24,26]. To obtain a unified model of *E. coli* RNA Pol elongation, it will be necessary to address the fact that the lifetime of the shortest pauses is comparable to the typical bandwidth of optical tweezers (both are ~1 second): either the experimental spatiotemporal resolution must be further increased, or more accurate analysis methods that can reliably distinguish pauses from elongation steps must be implemented. In both cases, increasing the size of data sets collected by single-molecule experiments will permit more stringent tests of different models[25,30,31].

Follow-up *in vitro* studies with optical tweezers have further investigated backtracking: for instance, transcription factors GreA and GreB, which cleave the protruding mRNA strand, were found to rescue backtracked RNA Pol[23], suggesting a possible proofreading mechanism. Additionally, the role of backtracking in the dynamics of eukaryotic polymerases has been investigated: work on RNA Pol II showed that its pause dynamics are dominated by backtracking to the extent that RNA Pol II cannot overcome forces beyond 8.5 pN[24]. Interestingly, the addition of TFIIS (a eukaryotic transcription factor that acts similarly to GreA and GreB) rescued backtracked RNA Pol II and permitted it to overcome forces of up to 16.5 pN. Finally, it has been shown that RNA Pol II backtracking becomes more likely in the vicinity of a roadblock such as a nucleosome[32] and that overcoming such a barrier requires the aid of thermal fluctuations. It is expected that the application of these *in vitro* single-molecule techniques will continue to shed light on the mechanistic details of how RNA Pol progresses in conjunction with the other factors involved in transcription.

To see whether similarly rich dynamics of RNA Pol occur *in vivo*, the dynamics of RNA Pol II in mammalian cells were studied by fluorescently labelling RNA Pol II and simultaneously monitoring an mRNA stem–loop that is specifically recognized by a GFP-labelled protein[33]. Using this approach, the authors observed that the rate-limiting step in transcription is the transition between initiation and elongation (RNA Pol II transcribed the complete gene in only one-ninetieth of cases) and that transcription is interrupted by long pauses that are probably related to backtracking. Although these long pauses are rare (only 4.2% of the polymerases are affected), they nonetheless have a substantial impact, as their cumulative duration can be to halve the total elongation time. Curiously, the pause-free elongation speed observed *in vivo* (~70 bp s^{-1} after the long pauses have been removed) was substantially higher than the corresponding value observed by *in vitro* (~15 bp s^{-1}). Whether this can be attributed to a lack of assisting transcription factors in *in vitro* assays or to the reduced temporal resolution of the *in vivo* experiments remains to be determined. Nonetheless, the *in vitro* and *in vivo* approaches yield complementary insights that are relevant for our understanding of this complex enzyme.

Termination. Optical tweezers have been useful for studying the different pathways underlying the termination of transcription[34]. By applying a force directly to the mRNA transcript generated by *E. coli* RNA Pol (FIG. 1Cb), it was possible to investigate the efficiency of termination for various termination sequences that encoded mRNA hairpins. Using this approach, it was determined that destabilization of the mRNA–DNA hybrid may be induced by a shearing mechanism induced by the hairpin. The degree of shearing, and hence the efficiency of termination, could be enhanced by shortening the hybrid, whereas it could be decreased through the presence of additional secondary structures that interfered with proper folding of the hairpin. However, we note that this result contradicts the results of a previous biochemical study[35] that suggested that the elongation complex is destabilized by the melting of 2 or 3 nucleotides upstream of the mRNA–DNA hybrid in the absence of any shearing. Further studies under applied loads may remain necessary to distinguish between these two models.

Thus, we see that optical tweezers can probe the activity of RNA Pol by using an application of force to perturb its local energy landscape, and smFRET studies report on the kinetics of molecular conformational changes. Integration of the two approaches is likely to be able to determine whether pausing is predominantly a template-related process or whether it is a direct consequence of conformational changes in the enzyme. Future efforts to unravel the dynamics of co-transcriptional phenomena such as translation or splicing warrant further application of single-molecule techniques.

Translation

Single-molecule approaches are useful for the study of movements within molecular complexes, as demonstrated by studies of structural changes in the *E. coli* ribosome. These structural rearrangements involve motions on a size scale that is perfectly suited to smFRET measurement[36], and this approach adds dynamic information to the structural snapshots deduced by X-ray crystallography or cryo-electron microscopy (cryo-EM). In addition, insights into the interaction of the *E. coli* ribosome with mRNA during elongation have been obtained using optical tweezers.

Initiation and elongation. To demonstrate how smFRET has enhanced our understanding of the motion of ribosomal subunits, we consider the results from three separate studies. In the first study[37], the two subunits of the *E. coli* ribosome (namely, 50S and 30S) were labelled with donor and acceptor dyes, respectively, and their interaction with initiation factor IF2 was studied. It was found that the association of the large subunit with the pre-initiation complex could be accelerated by IF2 by a factor of four. The authors determined that IF2 subsequently hydrolyses a single GTP to align the 30S subunit with the 50S subunit by rotating it with respect to the 50S. This rotation brings the ribosome into the elongation state. A related study[38] showed that this anticlockwise rotation did not require the presence of elongation factor G (EF-G), which supplies the necessary energy for

Elongation factor G
(EF-G). A factor that provides the bacterial ribosome with the necessary energy (derived from GTP hydrolysis) required to translocate along the mRNA.

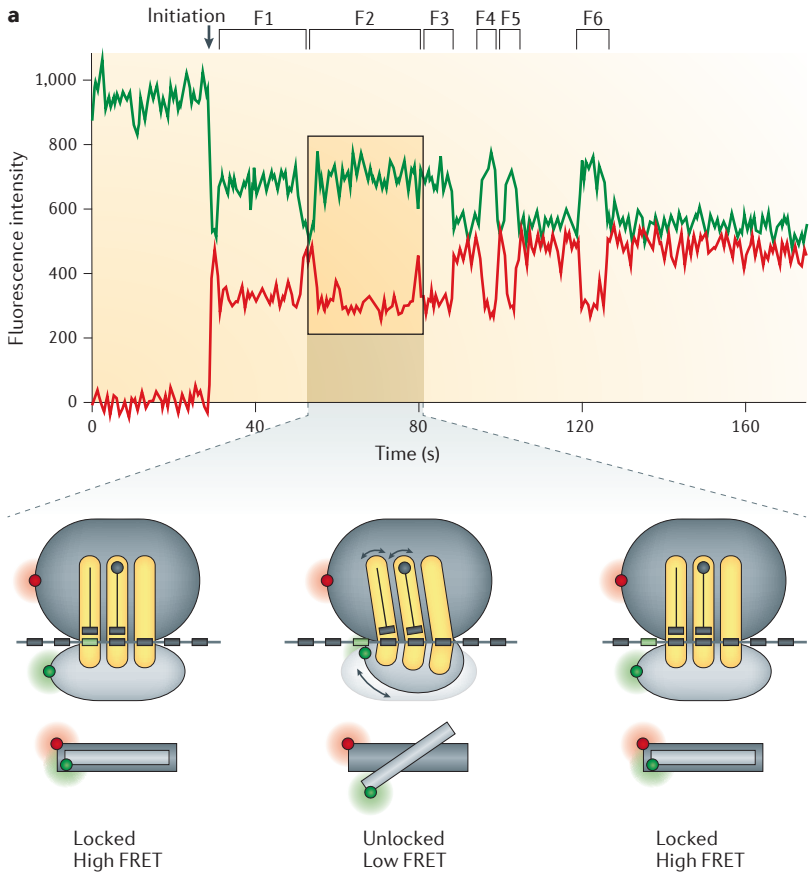

Figure 2 | **Studies of the ribosome and translation at the single-molecule level.** **a** | Study of the dynamics of the ribosomal subunits over multiple elongation cycles. The two ribosomal subunits are labelled with dyes for single-molecule Förster (fluorescence) resonance energy transfer (smFRET; small subunit labelled with donor, green circle; large subunit labelled with acceptor, red circle), as shown in the inset. A high signal in the green trace implies an increased distance between the dyes, and a high signal in the red trace implies a decreased distance. At the start of the experiment, the labelled 30S subunit is bound to the tethered mRNA, and the labelled 50S subunit is flushed into the flow cell. At *t* ~30 s, initiation is clearly visible by the first appearance of a signal from the acceptor dye (red trace). At each step of the elongation cycle, the rotation of the large subunit with respect to the small subunit was monitored, represented by the signal of the donor (green trace) and the acceptor (red trace). The accompanying mechanical motions within the ribosome are depicted in the inset from two perspectives: a side view showing the tRNA translocation and a bottom view in which subunit rotation is visible. The three yellow slots represent (from right to left) the ribosomal A, P and E sites. **b** | A schematic of a force spectroscopy study of ribosome translation dynamics. Here, the ribosome unwinds and translates an mRNA hairpin held at its extremities by two beads, one of which is maintained in an optical trap. Panel **a** is modified, with permission, from REF. 39 © (2008) Macmillan Publishers Ltd. Panel **b** is modified, with permission, from REF. 41 © Macmillan Publishers Ltd. All rights reserved.

ribosome translocation via GTP hydrolysis. The rotation itself is thermally driven, but it is stabilized in a pre-translocation (that is, rotated or 'unlocked') state by EF-G binding after peptide bond formation. Subsequent GTP hydrolysis by EF-G propels the ribosome into the 'locked' (non-rotated) state to drive ribosome translocation. A third smFRET experiment then demonstrated multiple cycles of high-to-low FRET efficiency in a single trace[39], reflecting the successive anticlockwise rotations of the 30S subunit with respect to the 50S subunit required to incorporate multiple amino acids (FIG. 2a). These observations are in accordance with structural information from cryo-EM studies and with additional smFRET studies that used the fluctuations in the positions of labelled tRNA within the ribosome as their readout[40].

The direct observation of translocation by the ribosomal molecular motor during elongation has been a longstanding challenge. It was overcome by using an optical tweezers assay that exploited the ability of the *E. coli* ribosome to unwind mRNA hairpins[41] (FIG. 2b), and it demonstrated that the elongation velocity is strongly influenced by the stability of the mRNA secondary structure. More recent investigations by the same group using hairpins with a differing GC content showed that the ribosome uses two distinct mechanisms: interaction of ribosomal proteins S3 and S4 with the mRNA backbone opens weak secondary structures, whereas a lever mechanism involving a tRNA–mRNA interaction and GTP hydrolysis (supplied by EF-G) opens strong secondary structures, as previously suggested by cryo-EM studies[42]. Detailed knowledge of the unwinding mechanism of the ribosome is important in the context of ribosomal frame shifting, in which interactions between the ribosome and particular mRNA sequences shift the mRNA reading frame by a single nucleotide. Investigation of frame shifting will thus provide a natural follow-up to these studies.

Recently, it has become possible to observe ribosomal elongation by fluorescence detection, using zero-mode waveguides (ZMWs) (see panel **a** of the figure in BOX 2) to detect individual labelled tRNAs above background fluorescence at physiological concentration[43]. Using this approach, the *E. coli* ribosome was tethered at the bottom of the ZMW by an mRNA template[44], and three different tRNAs (namely, lysine-tRNA, phenylalanine-tRNA and *N*-formylmethionine-tRNA) were labelled with different colours. Because a ribosome must contain the $tRNA^{fMet}$ to enter elongation, detection of its associated colour could identify tethered ribosomes in the ZMW. Subsequent incorporation of the other two labelled amino acids was then monitored by measuring the dwell times of tRNAs in the ribosome for a total of 12 amino acid incorporation events. Interestingly, the authors observed that the ribosomal A and E sites almost never simultaneously contain a tRNA: most frequently, only the A and P sites contain tRNAs, as the exit of a tRNA from the ribosome occurs rapidly after translocation has taken place[45]. Future studies could use the ZMW approach together with labelled tRNA to observe more complex tRNA dynamics: for

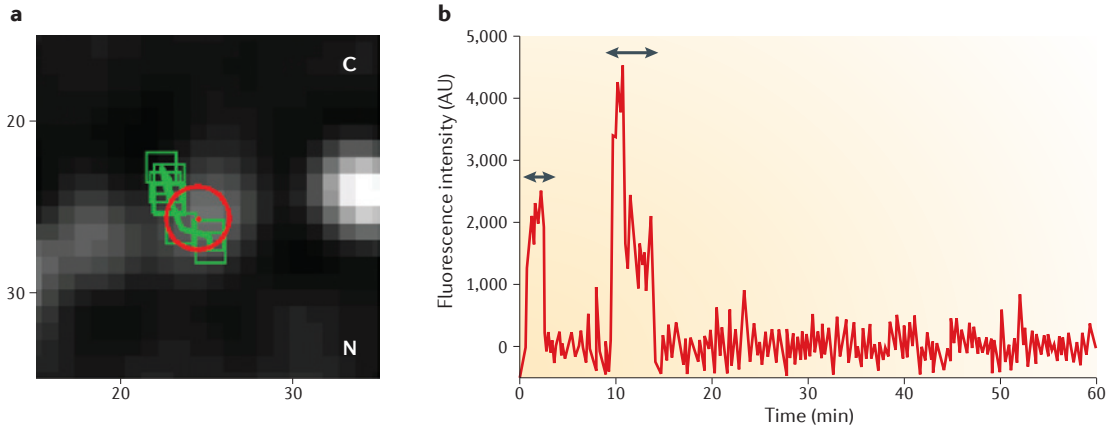

Figure 3 | **Observations of nuclear export and splicing at the single-molecule level.** **a** | Following mRNA export from the nucleus by super-registration microscopy. Tracked positions of β-actin mRNA labelled by multiple copies of YFP fused to a MS2 protein tag (in green) overlaid on the position of the nuclear pore complex (NPC) scaffold protein POM121 labelled with tandem Tomato fluorescent protein (in red). 'N' denotes the nucleus, and 'C' denotes the cytoplasm. Axes are in pixel units, and each pixel represents 64 nm. **b** | Ordered and dynamic assembly of spliceosomes. Shown here is a single-molecule fluorescence trace of labelled spliceosome subcomplexes U1. The trace reveals multiple binding and dissociation events to precursor mRNA that was colocalized (not shown), suggesting reversible binding. The arrows indicate the duration of binding events that can be analysed to determine the lifetimes. Similar traces were obtained for U2, U5 and the multiprotein Prp19 complex. Panel **a** is modified, with permission, from REF. 53 © (2010) Macmillan Publishers Ltd. All rights reserved. Panel **b** is modified, with permission, from REF. 56 © (2011) American Association for the Advancement of Science.

example, during frame shifting or in the presence of high concentrations of acylated tRNAs.

Termination and protein folding. Translation termination is a multi-step process involving numerous factors for which the dynamics have been studied using smFRET. Such experiments have provided detailed mechanistic insights into the association of release factors with the *E. coli* ribosome and into the specific position of the large ribosomal subunit with respect to the small subunit at each step of termination[46]. The influence of the ribosome on protein folding has also been the subject of a recent single-molecule study[47]. To study protein folding in the presence of the *E. coli* ribosome, the authors attached the ribosome to a bead held in a micropipette (see panel **d** of the figure in BOX 1). In the presence of an *in vitro* translation system, this ribosome synthesized T4 lysozyme, which was then coupled to an optically trapped bead via a DNA handle. By comparing the observed folding pathway to identical experiments carried out in the absence of the ribosome, the influence of the ribosome on the folding pathway was assessed. Interestingly, although the presence of the ribosome reduced both the overall rate (down by more than 100-fold) and the overall yield of folded lysozyme (down nearly fourfold), the lysozymes that did fold assumed a more compact form. Thus, the authors concluded that the ribosome acts as a chaperone that slowly guides the proteins into properly folded structures.

Splicing and export

In eukaryotes, many RNAs need to be exported out of the nucleus: for example, for translation in the cytoplasm. Single-molecule studies have begun to reveal properties of transport through the nuclear pore complex in permeabilized cells[48–50] and of the individual nucleoporins *in vitro*[51,52]. For example, a two-colour super-registration microscopy approach was used to track mRNA transport *in vivo*[53] (FIG. 3a). Interesting observations included the finding that individual mRNA molecules often scan multiple pores before being exported and that not all nuclear pore complexes (NPCs) are equally active in mRNA export. The authors were able directly to observe individual mRNAs being exported from the nucleus and to propose a kinetic model for export that suggests that docking to and release from the NPC, rather than transport through the central channel, are the rate-limiting steps[53].

Several single-molecule studies of splicing, including of self-splicing introns, have used purified components and have revealed the dynamics of individual steps in splicing[54,55]. In a recent study, individual spliceosomal subcomplexes were labelled in yeast whole-cell extract with different organic dyes, and using multicolour TIRF microscopy[56] (BOX 2), the authors studied their assembly on fluorescently labelled, surface-immobilized precursor mRNA (pre-mRNA) constructs (FIG. 3b). They were able to deduce the order and kinetics of spliceosome assembly and found that the assembly steps are reversible and that the assembly rates of the different components are similar, such that no particular step is strongly rate-limiting. In the future, single-molecule methods have great potential to reveal further details of the various splicing pathways, including alternative splicing[57,58].

Nuclear export and splicing both involve very large (>MDa) and complex protein or nucleoprotein assemblies (namely, the NPC and the spliceosome,

Ribosomal A, P and E sites
The aminoacyl, peptidyl and exit sites of the ribosome, respectively, which are the three different binding sites of tRNAs.

Nucleoporins
Proteins that comprise the nuclear pore complex.

Super-registration microscopy
The use of fluorescence microscopy to localize fluorescent probes as described in Box 2 in a way that accurately registers the relative positions of labels that fluoresce in different colours.

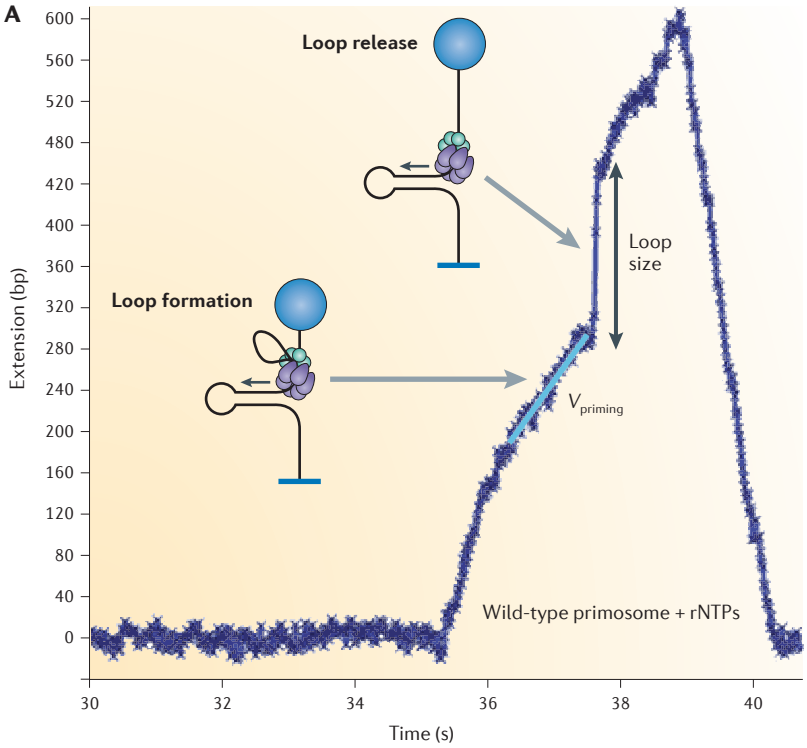

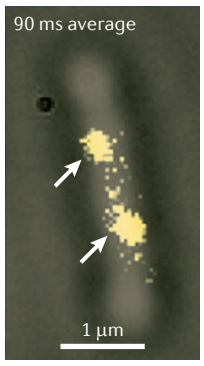

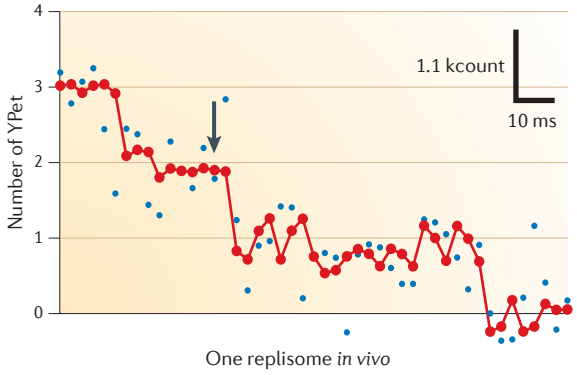

Figure 4 | **Replisome architecture and dynamics.** **A** | Looping of DNA during primer synthesis and unwinding. Here, an experimental trace is shown from which the priming velocity and loop size can be inferred. A magnetic tweezer is used, and the changes in DNA length are measured. **B** | Stoichiometry of replisome components. **Ba** | An overlay of bright-field (grey) and fluorescence images (yellow) of an *E. coli* strain with one of the replisome components fluorescently labelled. **Bb** | Photobleaching traces of fluorescent proteins in living *E. coli* indicating the presence of a single replisome. The arrow indicates 45 ms. rNTP, ribonucleotide triphosphate. $V_{priming}$, unwinding velocity during primer synthesis. Panel **A** is modified, with permission, from REF. 65 © (2009) Macmillan Publishers Ltd. All rights reserved. Panel **B** is modified, with permission, from REF. 77 © (2010) American Association for the Advancement of Science.

respectively) that pose substantial challenges to traditional high-resolution structure techniques and bulk biochemical assays. Overcoming these challenges and resolving the dynamics of these complex mechanochemical machines will continue to require new experimental approaches at the single-molecule level.

Replication

The different enzymes that act in concert to carry out DNA synthesis are collectively known as the replisome[59–61]. The architectural complexity of the replisome varies and encompasses four different proteins in bacteriophage T7 (REF. 62), eight proteins in bacteriophage T4 (REF. 62), twelve in *E. coli*[63] and even more in eukaryotes[63]. Our understanding of replisome dynamics has benefited from studies at the single-molecule level. *In vitro*, it has been possible to investigate the motor activity of individual polymerases[64] or individual helicases[65–67] using magnetic or optical tweezers (BOX 1). In a recent study[68], a combination of fluorescence spectroscopy together with optical trapping was used to investigate the polymerization of single-strand binding protein (SSB), which has a key role in lagging strand replication. More recently, it has also become possible to study the activity of complete replisomes *in vitro* at the single-molecule level, relying on either direct reconstitution (for phage T4 (REF. 69), phage T7 (REF. 70) and *E. coli*[71]) or the use of cell extracts (for eukaryotic systems[72]). Such studies of complete biological complexes should facilitate comparison with *in vivo* experiments.

Replication dynamics. To show how *in vitro* single-molecule assays can be used to probe the dynamics of replication, we briefly describe three recent studies that have focused on the interplay between helicase activity and primase activity. During replication, new primers need to be continuously synthesized to generate Okazaki fragments. The ssDNA template used for priming is formed by the helicase as it unwinds duplex DNA. However, the primase synthesizes RNA primers in the opposite direction to fork progression. Three possible ways to coordinate this process have been suggested: pausing (which would lead to a cessation of unwinding); DNA looping (which would result from continued synthesis by both helicase and primase while they remain associated); and disassembly (in which primase and helicase dissociate from one another). A short DNA hairpin tethered in magnetic tweezers was used to investigate these models for the T4 primosome, in which the helicase and primase are thought to associate. For a given applied force, changes in the length of the DNA molecule provide information about changes in its conformation caused by the primosome complex. It was found that the T4 primosome uses both the disassembly and DNA looping mechanisms and has a preference for the latter in the context of a full replisome (FIG. 4A). Two other studies, which investigated priming dynamics for the T7 replisome, used a flow-stretching assay[70] and smFRET[73], respectively. These studies revealed partially conflicting results. The flow-stretching assay study indicated that the primase slows down leading-strand synthesis sufficiently to allow lagging-strand synthesis to keep up. However, the smFRET study concluded that the leading strand T7 replisome did not pause (in contrast to the observations in the flow-stretching assay study), that the leading strand synthesis is slower than the lagging strand synthesis, and that priming loops are formed on the lagging strand.

Replisome stoichiometry. Both *in vitro* and *in vivo* single-molecule studies have recently shed new light on replisome stoichiometry. In a study using purified proteins[74], it was proposed that the DNA Pol III holoenzyme contains three DNA Pol III cores — this was in contrast to earlier models that suggested there were only two (bound at the leading and lagging strands, respectively)[75]. Relying on the ability to localize individual DNA-bound fluorescent proteins inside living cells[76] (BOX 2), ten different components of the replisome were fluorescently labelled in separate *E. coli* strains [77] (FIG. 4Ba). Analysis of the number of bleaching events (whereby each event is generated by a single labelled molecule) and their intensities allows determination of the number of molecules that are present within a diffraction-limited spot (FIG. 4Bb), and this enabled the authors to conclude that the *E. coli* replisome contains three DNA Pol III cores. More recent *in vivo* work has confirmed the observation of three DNA Pol III cores, with the caveat that the binding of the third polymerase appeared to be transient[78]. A potential function for a third polymerase was investigated by using a single-molecule flow-stretching assay (see panel **d** of the figure in BOX 1) together with a bulk bead-based assay[79]. The authors observed that a tripolymerase (tri-DNA Pol) replisome is more efficient at lagging-strand synthesis than its dipolymerase (di-DNA Pol) counterpart (ssDNA gaps were observed in the di-DNA Pol case) and that it also displays increased processivity. That is, the DNA fragments generated by the tri-DNA Pol were nearly twice as long as those from the di-DNA Pol. From these *in vivo* and *in vitro* data, the presence of a third polymerase seems plausible, but further investigations are necessary to exclude other models and to determine the exact role of such a third polymerase *in vivo*[80].

Challenges and future directions

What are the most interesting challenges that remain in our understanding of genomic processes? And how will single-molecule techniques continue to contribute to them? Will some single-molecule techniques become as commonplace as gel electrophoresis?

Challenges in molecular mechanisms. Many challenges remain in understanding genome processing at the molecular level. For example, although many molecular processes studied using single-molecule force spectroscopy have involved the motion of molecular motors along a linear template, the double-stranded helical nature of DNA also means that there are important roles for rotary motion. For example, the unwinding activity of replisomes or RNA Pol proteins generates torsional stress in the DNA template, and sometimes this may not be dissipated sufficiently rapidly by topoisomerases (reviewed in REF. 81). By analogy to the way in which force–velocity relationships have shed light on the mechanochemistry of linear motion, the measurement of torque–angular velocity relations can be used to investigate the mechanochemistry of rotary motion for polymerases, helicases and other genome-processing enzymes. Such investigations will be facilitated by the recent introduction of measurement techniques that report on torque and twist, such as magnetic torque tweezers[82–86].

A separate challenge at the molecular level is to understand how the conformational dynamics of a molecular motor are linked to any physical displacement it executes along a DNA or RNA track. Single-molecule fluorescence techniques such as FRET (BOX 2) are ideal for the study of the nanometre-scale conformational changes that proteins undergo. To correlate these (internal) changes with physical displacement along the track of the motor, a feasible approach is the integration of fluorescence spectroscopy with force spectroscopy. Initial efforts along these lines have been published[87–89]. In addition to monitoring the conformational changes of an enzyme during translocation along a DNA track, such approaches could concurrently investigate the coordination of ATP hydrolysis.

Increasing complexity. An ongoing challenge is to apply *in vitro* single-molecule techniques to increasingly complex biological systems. As well as investigating single molecular motors in isolation, motors can be studied as a part of reconstituted protein complexes, as in the case of DNA replication. Alternatively, the interplay between different types of molecular motors could be studied, as in the coordination between transcription and translation. The influence of more complex substrates (such as chromatin) and their influence on genomic processing is another interesting challenge. A possible approach is to examine protein activity in cell extracts[56,72,90], whereby the proteins of interest will have the appropriate post-translational modifications and native binding partners. However, technical challenges, such as unwanted fluorescence background or unwanted adsorption will need to be overcome. An alternative approach towards studying protein assemblies consists of purifying molecular complexes by immunoprecipitation and selectively adsorbing them onto surfaces for *in vitro* analysis[91,92]. This could improve understanding of molecular assemblies, such as the RNA-induced silencing complex (RISC) and proteins grouped onto telomeres.

Single-molecule techniques could also be harnessed to investigate genome processing over a much wider range of sequences than would typically be considered, potentially up to full genomic coverage. At present, this is the case for single-molecule DNA sequencing, in which genome sequences are determined by single-molecule fluorescence measurements of a large number of genome segments in parallel. Potentially, different parts of the genome could be interrogated at the single-molecule level to ascertain details such as their mechanical properties, transcription efficiency and transcription dynamics through single-molecule force spectroscopy or single-molecule fluorescence, or a combination thereof. These investigations and those of more complex biological systems discussed in the previous paragraph benefit from increased parallelization of single-molecule readouts. In certain approaches, such as TIRF microscopy, parallel readout is already the standard approach, but in other approaches, such as magnetic tweezers, it has only recently become more widely available[93].

Mechanochemical
A description of how the chemical reactions driving biological processes, such as ATP hydrolysis in a molecular motor, are coupled to mechanical motion: for example, translocation along a nucleic acid template.

Primosome
A protein complex consisting of a helicase and primase that is responsible for the synthesis of RNA primers during DNA replication.

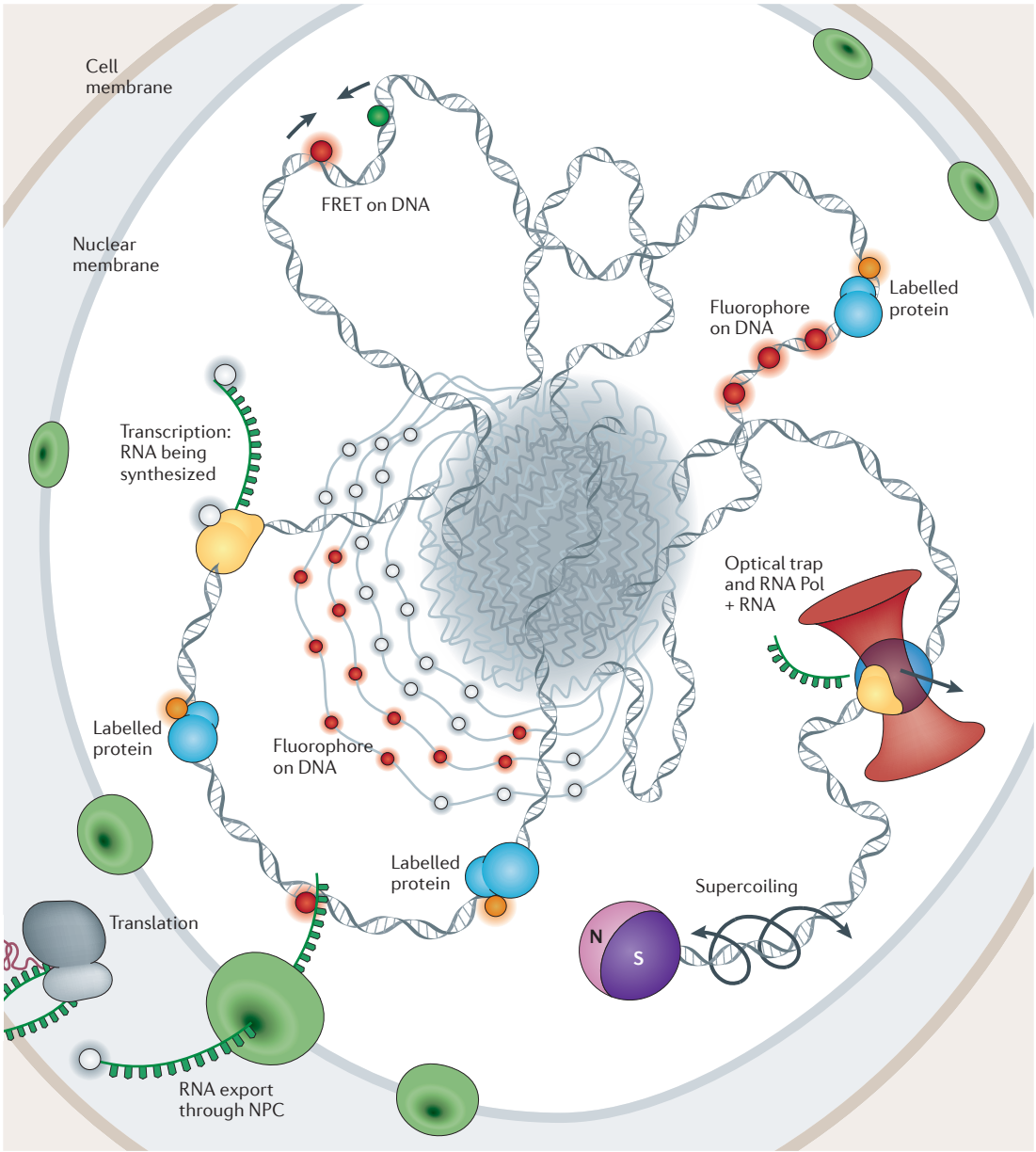

Figure 5 | **Genome processing taking place inside a cell nucleus and potential ways of monitoring it at the single-molecule level.** A schematic view (not to scale) inside the nucleus showing DNA in various stages of condensation being acted on by molecular motors, such as RNA polymerase (RNA Pol) and the replisome, and various potential ways of probing the genome, as well as processing of the genome by single-molecule techniques. FRET, Förster (fluorescence) resonance energy transfer; NPC, nuclear pore complex.

Studies of living cells. Given that genomic processing in its full complexity occurs in the context of living cells, the ultimate goal is to observe and to manipulate molecular processes *in vivo* at high spatial and temporal resolution. To demonstrate some of the possibilities, FIG. 5 depicts a range of genomic interactions that take place in and around the nucleus of a eukaryotic cell together with ways in which they might be probed using single-molecule methods. The DNA itself has an overall architecture that depends on the state of the cell cycle; a rapid and detailed series of snapshots of the entire architecture would be of great interest to facilitate understanding of, for example, the influence of architecture on transcriptional patterns. Already, fluorescence spectroscopy has been used for spatial calibration of chromosome capture data to aid mapping of the three-dimensional architecture of the *Caulobacter crescentus* genome[94]. Super-resolution microscopy has made it possible to resolve the architecture of the bacterial genome in fixed cells to better than 100 nm[95], and there will no doubt be further improvements. It could also be of interest to monitor local stress and strain in DNA intracellularly; a FRET sensor integrated into the DNA could potentially fulfil such a role.

RNA aptamers
RNA molecules that specifically bind to a target molecule.

Of similar importance is the monitoring of RNA and proteins *in vivo*. RNA is typically visualized by fluorescence *in situ* hybridization (FISH), which can be carried out at the single-molecule level[96] or by detection of RNA-bound proteins[97]. However, a recent interesting development is the generation of genetically encodable RNA aptamers that can directly bind fluorescent dyes[98]. Building on the ability to image protein dynamics intracellularly at the single-molecule level, multicolour imaging of different proteins could potentially reveal the dynamics of network interactions. For example, recent work has made it possible to image DNA-binding proteins in the bacterial nucleoid at a high resolution[99,100]. A similar approach could help to elucidate chromatin structure in live cells: for example, by labelling histone proteins. However, for *in vivo* imaging in particular, an ongoing challenge is to improve the ease and specificity of introducing fluorescent labels and to enhance their photon yield[101].

Another area for development is monitoring and applying forces or torques within the cell (FIG. 5). To date, force measurements on living cells have typically focused on the forces exerted by structures that execute large-scale motion — such as the filopodia involved in cell migration[102] — which allows measurement to be carried out using atomic force microscopy[103] or the deflection of microfabricated pillars[104–106]. Intracellular force measurements are more challenging[107,108] but can be achieved through the introduction of micron- or submicron-sized particles[109,110] or careful design of calibrated fluorescent probes[111–113]. In the future, more mature versions of these approaches might be applied to genome-processing events. Finally, it will be very interesting to monitor the extent to which genome processing is sensitive to external mechanical perturbations[114]; this could be examined using a combination of mechanical manipulation through single-molecule force spectroscopy and intranuclear readout through fluorescence imaging.

Ultimately, our understanding of the genome and its processing will rely on input from both *in vitro* and *in vivo* techniques and from many fields: biology, bioinformatics, chemistry, physics, engineering, nanoscience and nanotechnology, to name a few. Merging such knowledge into an understanding of cellular function will occupy us for decades to come.

1. Pareek, C. S., Smoczynski, R. & Tretyn, A. Sequencing technologies and genome sequencing. *J. Appl. Genet.* **52**, 413–435 (2011).
2. Forget, A. L. & Kowalczykowski, S. C. Single-molecule imaging brings Rad51 nucleoprotein filaments into focus. *Trends Cell Biol.* **20**, 269–276 (2010).
3. Finkelstein, I. J. & Greene, E. C. Single molecule studies of homologous recombination. *Mol. Biosyst.* **4**, 1094–1104 (2008).
4. Vinograd, J., Lebowitz, J., Radloff, R., Watson, R. & Laipis, P. The twisted circular form of polyoma viral DNA. *Proc. Natl Acad. Sci. USA* **53**, 1104–1111 (1965).
5. Sebring, E. D., Kelly, T. J. Jr, Thoren, M. M. & Salzman, N. P. Structure of replicating simian virus 40 deoxyribonucleic acid molecules. *J. Virol.* **8**, 478–490 (1971).
6. Ostrander, E. A., Benedetti, P. & Wang, J. C. Template supercoiling by a chimera of yeast GAL4 protein and phage T7 RNA polymerase. *Science* **249**, 1261–1265 (1990).
7. Neher, E. & Sakmann, B. Patch clamp techniques for studying ionic channels in excitable membranes. *Annu. Rev. Physiol.* **46**, 455–472 (1984).
8. Orrit, M. & Bernard, J. Single pentacene molecules detected by fluorescence excitation in a *p*-terphenyl crystal. *Phys. Rev. Lett.* **65**, 2716–2719 (1990).
9. Betzig, E. & Chichester, R. J. Single molecules observed by near-field scanning optical microscopy. *Science* **262**, 1422–1425 (1993).
10. Chalfie, M., Tu, Y., Euskirchen, G., Ward, W. W. & Prasher, D. C. Green fluorescent protein as a marker for gene expression. *Science* **263**, 802–805 (1994).
11. Wang, M. D. *et al.* Force and velocity measured for single molecules of RNA polymerase. *Science* **282**, 902–907 (1998).
12. Dutta, D., Shatalin, K., Epshtein, V., Gottesman, M. E. & Nudler, E. Linking RNA polymerase backtracking to genome instability in *E. coli*. *Cell* **146**, 533–543 (2011).
13. Koster, D. A., Croquette, V., Dekker, C., Shuman, S. & Dekker, N. H. Friction and torque govern the relaxation of DNA supercoils by eukaryotic topoisomerase IB. *Nature* **434**, 671–674 (2005).
14. Bormuth, V., Varga, V., Howard, J. & Schaffer, E. Protein friction limits diffusive and directed movements of kinesin motors on microtubules. *Science* **325**, 870–873 (2009).
15. Schafer, D. A., Gelles, J., Sheetz, M. P. & Landick, R. Transcription by single molecules of RNA polymerase observed by light microscopy. *Nature* **352**, 444–448 (1991).
16. Friedman, L. J. & Gelles, J. Mechanism of transcription initiation at an activator-dependent promoter defined by single-molecule observation. *Cell* **148**, 679–689 (2012).
This paper describes studies using an *in vitro* TIRF microscopy assay of the association and dissociation of the bacterial RNA Pol σ54 factor during the transition from initiation to elongation.
17. Kapanidis, A. N. *et al.* Initial transcription by RNA polymerase proceeds through a DNA-scrunching mechanism. *Science* **314**, 1144–1147 (2006).
This was the first *in vitro* experimental complete study showing the scrunching mechanism of RNA Pol initiation by smFRET.
18. Revyakin, A., Liu, C., Ebright, R. H. & Strick, T. R. Abortive initiation and productive initiation by RNA polymerase involve DNA scrunching. *Science* **314**, 1139–1143 (2006).
19. Treutlein, B. *et al.* Dynamic architecture of a minimal RNA polymerase II open promoter complex. *Mol. Cell* **46**, 136–146 (2012).
20. Abbondanzieri, E. A., Greenleaf, W. J., Shaevitz, J. W., Landick, R. & Block, S. M. Direct observation of base-pair stepping by RNA polymerase. *Nature* **438**, 460–465 (2005).
This paper reports the first force spectroscopy study of RNA Pol at the base-pair resolution, using optical tweezers.
21. Neuman, K. C., Abbondanzieri, E. A., Landick, R., Gelles, J. & Block, S. M. Ubiquitous transcriptional pausing is independent of RNA polymerase backtracking. *Cell* **115**, 437–447 (2003).
22. Herbert, K. M. *et al.* Sequence-resolved detection of pausing by single RNA polymerase molecules. *Cell* **125**, 1083–1094 (2006).
23. Shaevitz, J. W., Abbondanzieri, E. A., Landick, R. & Block, S. M. Backtracking by single RNA polymerase molecules observed at near-base-pair resolution. *Nature* **426**, 684–687 (2003).
24. Galburt, E. A. *et al.* Backtracking determines the force sensitivity of RNAP II in a factor-dependent manner. *Nature* **446**, 820–823 (2007).
25. Depken, M., Galburt, E. A. & Grill, S. W. The origin of short transcriptional pauses. *Biophys. J.* **96**, 2189–2193 (2009).
26. Mejia, Y. X., Mao, H., Forde, N. R. & Bustamante, C. Thermal probing of *E. coli* RNA polymerase off-pathway mechanisms. *J. Mol. Biol.* **382**, 628–637 (2008).
27. Zhou, J., Ha, K. S., La Porta, A., Landick, R. & Block, S. M. Applied force provides insight into transcriptional pausing and its modulation by transcription factor NusA. *Mol. Cell* **44**, 635–646 (2011).
28. Herbert, K. M. *et al. E. coli* NusG inhibits backtracking and accelerates pause-free transcription by promoting forward translocation of RNA polymerase. *J. Mol. Biol.* **399**, 17–30 (2010).
29. Dalal, R. V. *et al.* Pulling on the nascent RNA during transcription does not alter kinetics of elongation or ubiquitous pausing. *Mol. Cell* **23**, 231–239 (2006).
30. Maoileidigh, D. O., Tadigotla, V. R., Nudler, E. & Ruckenstein, A. E. A unified model of transcription elongation: what have we learned from single-molecule experiments? *Biophys. J.* **100**, 1157–1166 (2011).
31. Voliotis, M., Cohen, N., Molina-Paris, C. & Liverpool, T. B. Fluctuations, pauses, and backtracking in DNA transcription. *Biophys. J.* **94**, 334–348 (2008).
32. Hodges, C., Bintu, L., Lubkowska, L., Kashlev, M. & Bustamante, C. Nucleosomal fluctuations govern the transcription dynamics of RNA polymerase II. *Science* **325**, 626–628 (2009).
33. Darzacq, X. *et al. In vivo* dynamics of RNA polymerase II transcription. *Nature Struct. Mol. Biol.* **14**, 796–806 (2007).
34. Larson, M. H., Greenleaf, W. J., Landick, R. & Block, S. M. Applied force reveals mechanistic and energetic details of transcription termination. *Cell* **132**, 971–982 (2008).
35. Gusarov, I. & Nudler, E. The mechanism of intrinsic transcription termination. *Mol. Cell* **3**, 495–504 (1999).
36. Petrov, A. *et al.* Dynamics of the translational machinery. *Curr. Opin. Struct. Biol.* **21**, 137–145 (2011).
37. Marshall, R. A., Aitken, C. E. & Puglisi, J. D. GTP hydrolysis by IF2 guides progression of the ribosome into elongation. *Mol. Cell* **35**, 37–47 (2009).
38. Cornish, P. V., Ermolenko, D. N., Noller, H. F. & Ha, T. Spontaneous intersubunit rotation in single ribosomes. *Mol. Cell* **30**, 578–588 (2008).
39. Aitken, C. E. & Puglisi, J. D. Following the intersubunit conformation of the ribosome during translation in real time. *Nature Struct. Mol. Biol.* **17**, 793–800 (2010).
This study used smFRET to follow the inter-subunit conformation of the ribosome during translation in real time.
40. Munro, J. B., Altman, R. B., O'Connor, N. & Blanchard, S. C. Identification of two distinct hybrid state intermediates on the ribosome. *Mol. Cell* **25**, 505–517 (2007).
41. Wen, J. D. *et al.* Following translation by single ribosomes one codon at a time. *Nature* **452**, 598–603 (2008).
This was the first *in vitro* observation of translating ribosomes using single-molecule force spectroscopy.
42. Namy, O., Moran, S. J., Stuart, D. I., Gilbert, R. J. & Brierley, I. A mechanical explanation of RNA pseudoknot function in programmed ribosomal frameshifting. *Nature* **441**, 244–247 (2006).

43. Eid, J. *et al.* Real-time DNA sequencing from single polymerase molecules. *Science* **323**, 133–138 (2009).
44. Uemura, S. *et al.* Real-time tRNA transit on single translating ribosomes at codon resolution. *Nature* **464**, 1012–1017 (2010).
This paper provides a demonstration of the use of ZMW to study *in vitro* translation in the presence of a high concentration of labelled tRNAs.
45. Gao, Y. G. *et al.* The structure of the ribosome with elongation factor G trapped in the posttranslocational state. *Science* **326**, 694–699 (2009).
46. Sternberg, S. H., Fei, J., Prywes, N., McGrath, K. A. & Gonzalez, R. L. Jr. Translation factors direct intrinsic ribosome dynamics during translation termination and ribosome recycling. *Nature Struct. Mol. Biol.* **16**, 861–868 (2009).
47. Kaiser, C. M., Goldman, D. H., Chodera, J. D., Tinoco, I. Jr & Bustamante, C. The ribosome modulates nascent protein folding. *Science* **334**, 1723–1727 (2011).
48. Yang, W., Gelles, J. & Musser, S. M. Imaging of single-molecule translocation through nuclear pore complexes. *Proc. Natl Acad. Sci. USA* **101**, 12887–12892 (2004).
49. Kubitscheck, U. *et al.* Nuclear transport of single molecules: dwell times at the nuclear pore complex. *J. Cell Biol.* **168**, 233–243 (2005).
50. Lowe, A. R. *et al.* Selectivity mechanism of the nuclear pore complex characterized by single cargo tracking. *Nature* **467**, 600–603 (2010).
51. Milles, S. & Lemke, E. A. Single molecule study of the intrinsically disordered FG-repeat nucleoporin 153. *Biophys. J.* **101**, 1710–1719 (2011).
52. Kowalczyk, S. W. *et al.* Single-molecule transport across an individual biomimetic nuclear pore complex. *Nature Nanotechnol.* **6**, 433–438 (2011).
53. Grunwald, D. & Singer, R. H. *In vivo* imaging of labelled endogenous β-actin mRNA during nucleocytoplasmic transport. *Nature* **467**, 604–607 (2010).
This is a demonstration of tracking mRNA export through the nuclear pore in live cells using a super-registration approach.
54. Abelson, J. *et al.* Conformational dynamics of single pre-mRNA molecules during *in vitro* splicing. *Nature Struct. Mol. Biol.* **17**, 504–512 (2010).
55. Karunatilaka, K. S., Solem, A., Pyle, A. M. & Rueda, D. Single-molecule analysis of Mss116-mediated group II intron folding. *Nature* **467**, 935–939 (2010).
56. Hoskins, A. A. *et al.* Ordered and dynamic assembly of single spliceosomes. *Science* **331**, 1289–1295 (2011).
This is a comprehensive study of spliceosome assembly using cell extract and multicolour TIRF microscopy.
57. Waks, Z., Klein, A. M. & Silver, P. A. Cell-to-cell variability of alternative RNA splicing. *Mol. Syst. Biol.* **7**, 506 (2011).
58. Vargas, D. Y. *et al.* Single-molecule imaging of transcriptionally coupled and uncoupled splicing. *Cell* **147**, 1054–1065 (2011).
59. O'Donnell, M. Replisome architecture and dynamics in *Escherichia coli*. *J. Biol. Chem.* **281**, 10653–10656 (2006).
60. Bates, D. The bacterial replisome: back on track? *Mol. Microbiol.* **69**, 1341–1348 (2008).
61. Yao, N. Y. & O'Donnell, M. SnapShot: the replisome. *Cell* **141**, 1088–1088.e1 (2010).
62. Benkovic, S. J., Valentine, A. M. & Salinas, F. Replisome-mediated DNA replication. *Annu. Rev. Biochem.* **70**, 181–208 (2001).
63. Johnson, A. & O'Donnell, M. Cellular DNA replicases: components and dynamics at the replication fork. *Annu. Rev. Biochem.* **74**, 283–315 (2005).
64. Maier, B., Bensimon, D. & Croquette, V. Replication by a single DNA polymerase of a stretched single-stranded *DNA. Proc. Natl Acad. Sci. USA* **97**, 12002–12007 (2000).
65. Manosas, M., Spiering, M. M., Zhuang, Z., Benkovic, S. J. & Croquette, V. Coupling DNA unwinding activity with primer synthesis in the bacteriophage T4 primosome. *Nature Chem. Biol.* **5**, 904–912 (2009).
This is a thorough investigation of the T4 primosome activity on the single-molecule level.
66. Ribeck, N., Kaplan, D. L., Bruck, I. & Saleh, O. A. DNAB helicase activity is modulated by DNA geometry and force. *Biophys. J.* **99**, 2170–2179 (2010).
67. Johnson, D. S., Bai, L., Smith, B. Y., Patel, S. S. & Wang, M. D. Single-molecule studies reveal dynamics of DNA unwinding by the ring-shaped T7 helicase. *Cell* **129**, 1299–1309 (2007).
68. Zhou, R. *et al.* SSB functions as a sliding platform that migrates on DNA via reptation. *Cell* **146**, 222–232 (2011).
69. Manosas, M., Spiering, M. M., Ding, F., Croquette, V. & Benkovic, S. J. Collaborative coupling between polymerase and helicase for leading-strand synthesis. *Nucleic Acids Res.* **40**, 6187–6198 (2012).
70. Lee, J. B. *et al.* DNA primase acts as a molecular brake in DNA replication. *Nature* **439**, 621–624 (2006).
71. Tanner, N. A. *et al.* Single-molecule studies of fork dynamics in *Escherichia coli* DNA replication. *Nature Struct. Mol. Biol.* **15**, 170–176 (2008).
72. Yardimci, H., Loveland, A. B., Habuchi, S., van Oijen, A. M. & Walter, J. C. Uncoupling of sister replisomes during eukaryotic DNA replication. *Mol. Cell* **40**, 834–840 (2010).
73. Pandey, M. *et al.* Coordinating DNA replication by means of priming loop and differential synthesis rate. *Nature* **462**, 940–943 (2009).
74. McInerney, P., Johnson, A., Katz, F. & O'Donnell, M. Characterization of a triple DNA polymerase replisome. *Mol. Cell* **27**, 527–538 (2007).
75. Lovett, S. T. Polymerase switching in DNA replication. *Mol. Cell* **27**, 523–526 (2007).
76. Xie, X. S., Choi, P. J., Li, G. W., Lee, N. K. & Lia, G. Single-molecule approach to molecular biology in living bacterial cells. *Annu. Rev. Biophys.* **37**, 417–444 (2008).
77. Reyes-Lamothe, R., Sherratt, D. J. & Leake, M. C. Stoichiometry and architecture of active DNA replication machinery in *Escherichia coli*. *Science* **328**, 498–501 (2010).
This was the first paper that determined the stoichiometry of the replisome in the living cell using single-molecule techniques.
78. Lia, G., Michel, B. & Allemand, J. F. Polymerase exchange during Okazaki fragment synthesis observed in living cells. *Science* **335**, 328–331 (2012).
79. Georgescu, R. E., Kurth, I. & O'Donnell, M. E. Single-molecule studies reveal the function of a third polymerase in the replisome. *Nature Struct. Mol. Biol.* **19**, 113–116 (2012).
80. McHenry, C. S. D. N. A. Replicases from a bacterial perspective. *Annu. Rev. Biochem.* **80**, 403–436 (2011).
81. Koster, D. A., Crut, A., Shuman, S., Bjornsti, M. A. & Dekker, N. H. Cellular strategies for regulating DNA supercoiling: a single-molecule perspective. *Cell* **142**, 519–530 (2010).
82. Lipfert, J., Kerssemakers, J. W., Jager, T. & Dekker, N. H. Magnetic torque tweezers: measuring torsional stiffness in DNA and RecA-DNA filaments. *Nature Methods* **7**, 977–980 (2010).
83. Lipfert, J., Wiggin, M., Kerssemakers, J. W., Pedaci, F. & Dekker, N. H. Freely orbiting magnetic tweezers to directly monitor changes in the twist of nucleic acids. *Nature Commun.* **2**, 439 (2011).
84. Gore, J. *et al.* Mechanochemical analysis of DNA gyrase using rotor bead tracking. *Nature* **439**, 100–104 (2006).
85. Bryant, Z. *et al.* Structural transitions and elasticity from torque measurements on DNA. *Nature* **424**, 338–341 (2003).
86. La Porta, A. & Wang, M. D. Optical torque wrench: angular trapping, rotation, and torque detection of quartz microparticles. *Phys. Rev. Lett.* **92**, 190801 (2004).
87. Comstock, M. J., Ha, T. & Chemla, Y. R. Ultrahigh-resolution optical trap with single-fluorophore sensitivity. *Nature Methods* **8**, 335–340 (2011).
88. Hohng, S. *et al.* Fluorescence-force spectroscopy maps two-dimensional reaction landscape of the Holliday junction. *Science* **318**, 279–283 (2007).
89. Liu, R., Garcia-Manyes, S., Sarkar, A., Badilla, C. L. & Fernandez, J. M. Mechanical characterization of protein I in the low-force regime by electromagnetic tweezers/evanescent nanometry. *Biophys. J.* **96**, 3810–3821 (2009).
90. Yan, J. *et al.* Micromanipulation studies of chromatin fibers in *Xenopus* egg extracts reveal ATP-dependent chromatin assembly dynamics. *Mol. Biol. Cell* **18**, 464–474 (2007).
91. Yeom, K. H. *et al.* Single-molecule approach to immunoprecipitated protein complexes: insights into miRNA uridylation. *EMBO Rep.* **12**, 690–696 (2011).
92. Jain, A. *et al.* Probing cellular protein complexes using single-molecule pull-down. *Nature* **473**, 484–488 (2011).
93. Ribeck, N. & Saleh, O. A. Multiplexed single-molecule measurements with magnetic tweezers. *Rev. Sci. Instrum.* **79**, 094301 (2008).
94. Umbarger, M. A. *et al.* The three-dimensional architecture of a bacterial genome and its alteration by genetic perturbation. *Mol. Cell* **44**, 252–264 (2011).
95. Schoen, I., Ries, J., Klotzsch, E., Ewers, H. & Vogel, V. Binding-activated localization microscopy of DNA structures. *Nano Lett.* **11**, 4008–4011 (2011).
96. Raj, A., van den Bogaard, P., Rifkin, S. A., van Oudenaarden, A. & Tyagi, S. Imaging individual mRNA molecules using multiple singly labeled probes. *Nature Methods* **5**, 877–879 (2008).
97. Trcek, T. *et al.* Single-mRNA counting using fluorescent *in situ* hybridization in budding yeast. *Nature Protoc.* **7**, 408–419 (2012).
98. Paige, J. S., Wu, K. Y. & Jaffrey, S. R. RNA mimics of green fluorescent protein. *Science* **333**, 642–646 (2011).
99. Lee, S. F., Thompson, M. A., Schwartz, M. A., Shapiro, L. & Moerner, W. E. Super-resolution imaging of the nucleoid-associated protein HU in *Caulobacter crescentus*. *Biophys. J.* **100**, L31–L33 (2011).
100. Wang, W., Li, G. W., Chen, C., Xie, X. S. & Zhuang, X. Chromosome organization by a nucleoid-associated protein in live bacteria. *Science* **333**, 1445–1449 (2011).
101. Fernandez-Suarez, M. & Ting, A. Y. Fluorescent probes for super-resolution imaging in living cells. *Nature Rev. Mol. Cell Biol.* **9**, 929–943 (2008).
102. Eyckmans, J., Boudou, T., Yu, X. & Chen, C. S. A hitchhiker's guide to mechanobiology. *Dev. Cell* **21**, 35–47 (2011).
103. Muller, D. J. & Dufrene, Y. F. Force nanoscopy of living cells. *Curr. Biol.* **21**, R212–R216 (2011).
104. Legant, W. R. *et al.* Microfabricated tissue gauges to measure and manipulate forces from 3D microtissues. *Proc. Natl Acad. Sci. USA* **106**, 10097–10102 (2009).
105. Xie, C., Hanson, L., Cui, Y. & Cui, B. Vertical nanopillars for highly localized fluorescence imaging. *Proc. Natl Acad. Sci. USA* **108**, 3894–3899 (2011).
106. Zhang, J. Microsystems for cellular force measurement: a review. *J. Micromech. Microeng.* **21**, 054003 (2011).
107. Dufrene, Y. F. *et al.* Five challenges to bringing single-molecule force spectroscopy into living cells. *Nature Methods* **8**, 123–127 (2011).
108. Wang, Y., Meng, F. & Sachs, F. Genetically encoded force sensors for measuring mechanical forces in proteins. *Commun. Integr. Biol.* **4**, 385–390 (2011).
109. Sims, P. A. & Xie, X. S. Probing dynein and kinesin stepping with mechanical manipulation in a living cell. *ChemPhysChem* **10**, 1511–1516 (2009).
110. Celedon, A., Hale, C. M. & Wirtz, D. Magnetic manipulation of nanorods in the nucleus of living cells. *Biophys. J.* **101**, 1880–1886 (2011).
111. Hu, S. *et al.* Intracellular stress tomography reveals stress focusing and structural anisotropy in cytoskeleton of living cells. *Am. J. Physiol. Cell Physiol.* **285**, C1082–C1090 (2003).
112. Grashoff, C. *et al.* Measuring mechanical tension across vinculin reveals regulation of focal adhesion dynamics. *Nature* **466**, 263–266 (2010).
113. Meng, F. & Sachs, F. Visualizing dynamic cytoplasmic forces with a compliance-matched FRET sensor. *J. Cell Sci.* **124**, 261–269 (2011).
114. Wang, N., Tytell, J. D. & Ingber, D. E. Mechanotransduction at a distance: mechanically coupling the extracellular matrix with the nucleus. *Nature Rev. Mol. Cell Biol.* **10**, 75–82 (2009).
115. Bustamante, C., Bryant, Z. & Smith, S. B. Ten years of tension: single-molecule DNA mechanics. *Nature* **421**, 423–427 (2003).
116. Greenleaf, W. J., Woodside, M. T. & Block, S. M. High-resolution, single-molecule measurements of biomolecular motion. *Annu. Rev. Biophys. Biomol. Struct.* **36**, 171–190 (2007).
117. Neuman, K. C. & Nagy, A. Single-molecule force spectroscopy: optical tweezers, magnetic tweezers and atomic force microscopy. *Nature Methods* **5**, 491–505 (2008).
118. Lipfert, J., Hao, X. & Dekker, N. H. Quantitative modeling and optimization of magnetic tweezers. *Biophys. J.* **96**, 5040–5049 (2009).
119. Strick, T. R., Allemand, J. F., Bensimon, D., Bensimon, A. & Croquette, V. The elasticity of a single supercoiled DNA molecule. *Science* **271**, 1835–1837 (1996).
120. van Oijen, A. M. & Loparo, J. J. Single-molecule studies of the replisome. *Annu. Rev. Biophys.* **39**, 429–448 (2010).

121. Butt, H. J., Cappella, B. & Kappl, M. Force measurements with the atomic force microscope: technique, interpretation and applications. *Surf. Sci. Rep.* **59**, 1–152 (2005).
122. Svoboda, K. & Block, S. M. Biological applications of optical forces. *Annu. Rev. Biophys. Biomol. Struct.* **23**, 247–285 (1994).
123. Moffitt, J. R., Chemla, Y. R., Smith, S. B. & Bustamante, C. Recent advances in optical tweezers. *Annu. Rev. Biochem.* **77**, 205–228 (2008).
124. Greenleaf, W. J., Woodside, M. T., Abbondanzieri, E. A. & Block, S. M. Passive all-optical force clamp for high-resolution laser trapping. *Phys. Rev. Lett.* **95**, 208102 (2005).
125. van Aelst, K. *et al.* Type III restriction enzymes cleave DNA by long-range interaction between sites in both head-to-head and tail-to-tail inverted repeat. *Proc. Natl Acad. Sci. USA* **107**, 9123–9128 (2010).
126. Snapp, E. L. Fluorescent proteins: a cell biologist's user guide. *Trends Cell Biol.* **19**, 649–655 (2009).
127. Ramanathan, S. P. *et al.* Type III restriction enzymes communicate in 1D without looping between their target sites. *Proc. Natl Acad. Sci. USA* **106**, 1748–1753 (2009).
128. Axelrod, D. Total internal reflection fluorescence microscopy in cell biology. *Traffic* **2**, 764–774 (2001).
129. Thompson, R. E., Larson, D. R. & Webb, W. W. Precise nanometer localization analysis for individual fluorescent probes. *Biophys. J.* **82**, 2775–2783 (2002).
130. Ram, S., Ward, E. S. & Ober, R. J. Beyond Rayleigh's criterion: a resolution measure with application to single-molecule microscopy. *Proc. Natl Acad. Sci. USA* **103**, 4457–4462 (2006).
131. Smith, C. S., Joseph, N., Rieger, B. & Lidke, K. A. Fast, single-molecule localization that achieves theoretically minimum uncertainty. *Nature Methods* **7**, 373–375 (2010).
132. Mortensen, K. I., Churchman, L. S., Spudich, J. A. & Flyvbjerg, H. Optimized localization analysis for single-molecule tracking and super-resolution microscopy. *Nature Methods* **7**, 377–381 (2010).
133. Hell, S. W. Microscopy and its focal switch. *Nature Methods* **6**, 24–32 (2009).
134. Patterson, G., Davidson, M., Manley, S. & Lippincott-Schwartz, J. Superresolution imaging using single-molecule localization. *Annu. Rev. Phys. Chem.* **61**, 345–367 (2010).
135. Tu, L. C. & Musser, S. M. Single molecule studies of nucleocytoplasmic transport. *Biochim. Biophys. Acta* **1813**, 1607–1618 (2011).

Acknowledgements
This work was supported by the European Science Foundation through a European Young Investigators (EURYI) grant to N.H.D. and by the Netherlands Organisation for Scientific Research through grants to N.H.D. and J.L. We thank anonymous referees for useful feedback and D. Grünwald for a critical reading of the manuscript. J. Kerssemakers is thanked for the visual layout of Figure 5. We acknowledge the many research efforts by groups in the field of genome processing and regret that owing to space limitations it was not possible to cite a larger number of high-quality works.

Competing interests statement
The authors declare no competing financial interests.

FURTHER INFORMATION
Nynke H. Dekker's homepage: http://nynkedekkerlab.tudelft.nl
ALL LINKS ARE ACTIVE IN THE ONLINE PDF